Reduction of Intrinsic Kinetic and Thermodynamic Barriers for Enzyme-catalyzed Proton Transfers from Carbon Acid Substrates

Stephen L. Bearne[‡,*] and Raymond J. Spiteri[§]

[‡]Department of Biochemistry and Molecular Biology, Halifax, Nova Scotia, B3H 1X5, Canada

[§]Department of Computer Science, University of Saskatchewan, Saskatoon, Saskatchewan, S7N 5A9, Canada

*   Author to whom correspondence should be addressed.

Phone: (902) 494-1974; fax: (902) 494-1355; e-mail: sbearne@dal.ca

Running Title: Enzyme-catalyzed Proton Transfers

Abstract

Many enzymes catalyze the heterolytic abstraction of the α-proton from a carbon acid substrate. Gerlt and Gassman have applied Marcus formalism to such proton transfer reactions to argue that transition states for concerted general acid-general base catalyzed enolization at enzyme active sites occur late on the reaction coordinate [Gerlt, J.A., Gassman, P.G. (1993) J. Am. Chem. Soc. 115, 11552-11568]. We postulate that as an enzyme evolves, it may decrease $\Delta G^{\ddagger}$ for a proton transfer step associated with substrate enolization by following the path of steepest descent on the two-dimensional surface corresponding to $\Delta G^{\ddagger}$, as defined by Marcus formalism. We show that for an enzyme that has decreased $\Delta G^{\ddagger}$ following the path of steepest descent, the values of the intrinsic kinetic ($\Delta G^{\ddagger}_{int,E}$) and thermodynamic ($\Delta G^{\circ}_{E}$) barriers for proton transfer reactions on the enzyme may be predicted from the known values of $\Delta G^{\ddagger}_{int,N}$ and ΔG°_{N} for the corresponding nonenzymatic reaction and the free energy of activation on the enzyme ($\Delta G^{\ddagger}_{E}$). In addition, the enzymatic transition state will occur later on the reaction coordinate than the corresponding nonenzymatic transition state (i.e., $x^{\ddagger}_{E} > x^{\ddagger}_{N}$) if the condition $\left(6 - \sqrt{2}\right)/8 < x^{\ddagger}_{N} < \left(6 + \sqrt{2}\right)/8$ is satisfied. For enzyme-catalyzed abstraction of the α-proton from carbon acid substrates with high pK_a values (e.g., $pK_a \sim 29$), the free energy of activation for the nonenzymatic reaction ($\Delta G^{\ddagger}_{N}$) is dominated by ΔG°_{N}. Reduction of $\Delta G^{\ddagger}$, via the path of steepest descent, will reduce ΔG° to a greater extent (i.e., differential binding) than $\Delta G^{\ddagger}_{int}$ if $\Delta G^{\circ}_{N} > 2\, \Delta G^{\ddagger}_{int,N}$.

1.   Introduction

Many enzymes catalyze the heterolytic abstraction of the α-proton from a carbon acid substrate to initiate 1,1-, 1,2-, and 1,3-migrations of protons, aldol and Claisen condensations, and β-elimination reactions (Richard and Amyes, 2001; Kluger, 1990; Gerlt, 1998). According to Marcus formalism (Albery, 1980; Cohen and Marcus, 1968; Marcus, 1969; Kresge and Silverman, 1999; Silverman, 2000), the free energy of activation ($\Delta G^{\ddagger}$) for such a unimolecular proton transfer reaction may be partitioned into two parts: (1) the thermodynamic barrier (ΔG°), and (2) the intrinsic kinetic barrier ($\Delta G^{\ddagger}_{int}$) as shown in equation 1 (where $|\Delta G^{\circ}| \leq 4\Delta G^{\ddagger}_{int}$) (Maskill, 1985).[FOOTNOTE 1] $\Delta G^{\ddagger}_{int}$ is the hypothetical activation barrier in the absence of a thermodynamic barrier (i.e., when $\Delta G^{\circ} = 0$). The Marcus formalism employed here describes the reaction coordinate as an inverted parabola and the free energy (G) at any point x on the reaction coordinate from substrate ($x = 0$) to product ($x = 1$) is related to ΔG° and $\Delta G^{\ddagger}_{int}$ as shown in equation 2. The position of the transition state on the reaction coordinate, $x^{\ddagger}$, corresponds to the maximum of the function given in equation 2 and is described by equation 3.

$$\Delta G^{\ddagger} = \Delta G^{\ddagger}_{int} + \frac{\Delta G^{\circ}}{2} + \frac{\left(\Delta G^{\circ}\right)^2}{16\Delta G^{\ddagger}_{int}} \tag{1}$$

$$G = -4\Delta G^{\ddagger}_{int}\left(x - 0.5\right)^2 + \Delta G^{\circ}\left(x - 0.5\right) \tag{2}$$

$$x^{\ddagger} = 0.5 + \frac{\Delta G^{\circ}}{8\Delta G^{\ddagger}_{int}} \tag{3}$$

Enzymes that catalyze the heterolytic abstraction of a proton adjacent to a carbonyl or carboxylic acid group (α-proton of a carbon acid substrate as shown in scheme 1) face two problems. First, the enol or enolate intermediate formed is unstable and poses a thermodynamic problem for the enzyme (Amyes and Richard, 1996; Chiang et al., 2000; Richard et al., 2002; Thibblin and Jencks, 1979). This problem may be overcome by stabilization of the intermediate (i.e., decreased ΔG°) through electrostatic stabilization and H-bonding interactions (Richard et al., 2002; Guthrie and Kluger, 1993). Second, the rate of nonenzymatic abstraction of the α-proton from a carbon acid is slower than the rate of abstraction of a proton from a heteroatom or normal acid (HX, where X = N, O, or S) of equal acidity because $\Delta G^{\ddagger}_{int}$ for proton abstraction from a carbon acid (~12 kcal/mol) is larger than that of a normal acid ($\leq$ 3 kcal/mol) (Albery, 1982; Chiang et al., 1988; Eigen, 1964; Bernasconi, 1992). This difference is thought to arise from changes in the orientations of solvent dipoles as the negative charge develops on the carbonyl oxygen

as the α-proton is abstracted (Bernasconi, 1992) and changes in the geometry of the carbon atom (Guthrie, 1998). Gerlt and Gassman (Gerlt and Gassman, 1993, 1993) pointed out that such solvent reorganization need not occur within an enzyme active site and that the judicious placement of an electrophilic catalyst adjacent to the carbonyl oxygen can stabilize the developing negative charge on the carbonyl oxygen thereby reducing the intrinsic kinetic barrier (i.e., $\Delta G^{\ddagger}_{int}$). In addition, the intrinsic kinetic barrier may also be reduced through concerted general acid catalysis (Gerlt and Gassman, 1993, 1993; Gerlt and Gassman, 1992; Gerlt et al., 1997).

<div align="center">INSERT: scheme 1 & Figure 1</div>

As an enzyme evolves to become a more proficient catalyst, how does it alter ΔG° and $\Delta G^{\ddagger}_{int}$, relative to each other, to achieve a significant reduction in $\Delta G^{\ddagger}$? Two proposals have been put forward to address this question (Figure 1). First, Albery, Knowles, and co-workers developed a general theory that relates the energetics of individual steps of an enzyme-catalyzed reaction to the catalytic efficiency of the enzyme (Albery and Knowles, 1977; Burbaum et al., 1989). According to their proposal, the catalytic efficiency of an enzyme may be improved during evolution in three stages in order of increasing difficulty: (1) "uniform binding", (2) "differential binding", and (3) "catalysis of an elementary step" (Burbaum et al., 1989; Albery and Knowles, 1976). Differential binding relates to the enzyme's ability to selectively bind a reactive intermediate relative to the substrate in the ground state, thereby decreasing the energy difference between the substrate and the intermediate (i.e., reduction of ΔG° as shown in Figures 1C and 1D). Such differential binding would equalize the relative energies of internal states (i.e., bound substrate and intermediate) giving an internal equilibrium constant (K_{int}) of approximately unity for enzymes that operate under reversible conditions (i.e., $\Delta G^{\circ} \approx 0$, see Figure 1D). (For irreversible enzymes, bound intermediate will be favored over bound substrate and $K_{int} > 1$ (Burbaum et al., 1989; Chin, 1983; Stackhouse et al., 1985).) Once differential binding has been optimized, an enzyme can only improve catalysis of an elementary step through selective stabilization of the transition state relative to the ground state (i.e., reduction of $\Delta G^{\ddagger}_{int}$).

In an alternative proposal, Gerlt, Gassman, and co-workers used Marcus formalism to argue that the transition state for concerted general acid-general base-catalyzed enzymatic proton transfers to and from carbon atoms adjacent to carbonyl or carboxyl groups (enolizations) occurs late on the reaction coordinate (Gerlt and Gassman, 1993, 1993; Gerlt and Gassman, 1992; Gerlt et al., 1991). Consequently, the

predicted value of K_{int} for the formation of the enolic(ate) intermediate from the substrate at the enzyme active site should be substantially less than unity (i.e., $\Delta G° > 0$, see Figure 1B). Although Gerlt and Gassman pointed out that the observed activation barriers for enzyme-catalyzed reactions could be achieved by lowering *both* $\Delta G°$ and $\Delta G^{\ddagger}_{int}$, they did not specify in what ratio these parameters might be altered. Herein, we use the activation free energy surface for a proton transfer reaction, as defined by Marcus formalism, to develop a quantitative theoretical description of how both $\Delta G°$ and $\Delta G^{\ddagger}_{int}$ might vary as the activation barrier on an enzyme is decreased along the path of steepest descent during evolution. In addition, we define conditions under which the enzymatic transition state will occur later on the reaction coordinate relative to the location of the corresponding nonenzymatic transition state.

2. Results and Discussion

Path of Steepest Descent. In terms of Marcus formalism, two possible extremes of enzyme evolution may be envisioned. First, an enzyme might improve its efficiency by reducing only $\Delta G^{\ddagger}_{int}$ (i.e., enhancing transition state stabilization) while having no effect on the thermodynamic barrier. For extremely endergonic reactions such as proton transfers from carbon acids, $\Delta G^{\ddagger}$ is dominated by $\Delta G°$, and reduction in $\Delta G^{\ddagger}_{int}$ alone cannot account for the observed rates of enzyme-catalyzed reactions (Gerlt, 1998). Second, an enzyme might improve its efficiency by reducing only $\Delta G°$ (i.e., enhancing differential binding) while having no effect on the intrinsic kinetic barrier. Certainly, it is unlikely that these two extreme mechanisms would operate in isolation since $\Delta G°$ and $\Delta G^{\ddagger}_{int}$ are not expected to be completely independent in an enzyme's active site. Structural features that reduce $\Delta G°$ may also produce reductions in $\Delta G^{\ddagger}_{int}$ and *vice versa*, especially if natural selection leads to the parsimonious use of catalytic groups at enzyme active sites (Gerlt and Gassman, 1993; Hanson and Rose, 1975). For example, the electrostatic interactions within a polar active site that stabilize the reactive intermediate (i.e., lower $\Delta G°$) may also serve to stabilize the transition state (Hammond, 1955) and to "solvate" the reactant so that solvent reorganization energies are reduced relative to those of the corresponding nonenzymatic reaction (i.e., lowering $\Delta G^{\ddagger}_{int}$) (Yadav et al., 1991).

Figure 2 shows the level curves of a contour plot for the two-dimensional activation free energy ($\Delta G^{\ddagger}$) surface for a proton transfer reaction as defined by $\Delta G^{\ddagger}_{int}$ and $\Delta G°$ according to equation 1. Assuming that proton transfer is rate-determining and that there is not a drastic change in mechanism, this

surface represents the values of $\Delta G^{\ddagger}$ that could be sampled as an enzyme evolves and catalysis of the proton transfer step is improved.[FOOTNOTE 2] A plausible evolutionary strategy for lowering $\Delta G^{\ddagger}$ is to follow the path of steepest descent from its value in the absence of enzyme ($\Delta G^{\ddagger}_{N}$) to its value on the enzyme ($\Delta G^{\ddagger}_{E}$). This path lowers both $\Delta G^{\ddagger}_{int}$ and ΔG° by the smallest amount each to yield the final value of $\Delta G^{\ddagger}_{E}$. Initially, mutations would generate enzymes with different values of $\Delta G^{\ddagger}_{E}$ that correspond to points on the activation free energy surface (i.e., ($\Delta G^{\ddagger}_{int,E}$, ΔG°_{E}, $\Delta G^{\ddagger}_{E}$)) that vary about the point ($\Delta G^{\ddagger}_{int,N}$, ΔG°_{N}, $\Delta G^{\ddagger}_{N}$) in a stochastic fashion. Those enzymes with combinations of $\Delta G^{\ddagger}_{int,E}$ and ΔG°_{E} that lie on or close to the path of steepest descent would have lower values of $\Delta G^{\ddagger}_{E}$ and therefore be favored by natural selection.

<center>**INSERT: Figure 2**</center>

Starting at the point ($\Delta G^{\ddagger}_{int,N}$, ΔG°_{N}) on the contour plot, the path of steepest descent can be calculated exactly using the implicit function given in equation 4 or approximately by following the path corresponding to the maximum directional derivative at small discrete intervals. (Equation 4 is the solution to differential equation 6.) The intersection of this path with the level curve corresponding to the value of $\Delta G^{\ddagger}_{E}$ gives the values of $\Delta G^{\ddagger}_{int,E}$ and ΔG°_{E} as shown in Figure 2.

$$f\left(\Delta G^{\ddagger}_{int}, \Delta G^{\circ}\right) = \ln \Delta G^{\ddagger}_{int} + f\left(\Delta G^{\ddagger}_{int,N}, \Delta G^{\circ}_{N}\right) - \ln \Delta G^{\ddagger}_{int,N} \tag{4}$$

where
$$f\left(\Delta G^{\ddagger}_{int}, \Delta G^{\circ}\right) = -(1/2)\ln\left|2 - \left(4\Delta G^{\circ}\big/\Delta G^{\ddagger}_{int}\right) + \left(\Delta G^{\circ}\big/\Delta G^{\ddagger}_{int}\right)^{2}\right| +$$
$$\left(1\ \sqrt{2}\right)\ln\left|\left(\left(\Delta G^{\circ}\big/\Delta G^{\ddagger}_{int}\right) - 2 - \sqrt{2}\right)\big/\left(\left(\Delta G^{\circ}\big/\Delta G^{\ddagger}_{int}\right) - 2 + \sqrt{2}\right)\right| \tag{5}$$

Changes in Transition State Location. We now delimit regions on the $\Delta G^{\ddagger}$ surface where lowering the value of $\Delta G^{\ddagger}$ from $\Delta G^{\ddagger}_{N}$ to $\Delta G^{\ddagger}_{E}$ along the path of steepest descent yields an enzymatic transition state that occurs either later or earlier on the reaction coordinate than the corresponding nonenzymatic transition state. Figure 3 shows examples of lines that intersect the level curves at values of $\Delta G^{\ddagger}_{int}$ and ΔG° that yield constant values of $x^{\ddagger}$. Setting the slope of such lines (i.e., $\Delta G^{\circ}/\Delta G^{\ddagger}_{int}$) equal to the gradient of the maximum directional derivative (equation 6) gives equation 7 (with $L = 0$). The two lines defined by equation 7 (with $L = 0$) partition the $\Delta G^{\ddagger}$ surface into three regions as indicated by the yellow and blue shading in Figures 2 and 3. Substitution of the roots of equation 7 with $L = 0$ (i.e., equation 8) into equation 3 gives the values of $x^{\ddagger}$ that correspond to this criterion (equation 9). In the regions shaded blue where $L > 0$ (i.e., $x^{\ddagger} < \left(6 - \sqrt{2}\right)\big/8$ and $x^{\ddagger} > \left(6 + \sqrt{2}\right)\big/8$), the path of steepest descent yields values of $\Delta G^{\ddagger}_{int,E}$ and ΔG°_{E} such that the location of the transition state for enzyme-catalyzed proton abstraction occurs

earlier on the reaction coordinate than does the corresponding transition state of the nonenzymatic reaction (i.e., $x^{\ddagger}_{E} < x^{\ddagger}_{N}$). However, in the region shaded yellow where $L < 0$ and $x^{\ddagger}$ satisfies condition 10, the path of steepest descent will yield values of $\Delta G^{\ddagger}_{int,E}$ and ΔG°_{E} that give $x^{\ddagger}_{E} > x^{\ddagger}_{N}$. This difference is more evident in Figure 3, which shows the gradient vectors at any given initial combination of $\Delta G^{\ddagger}_{int}$ and ΔG°, and their relation to lines defined by specific $\Delta G^{\circ}/\Delta G^{\ddagger}_{int}$ ratios (i.e., constant values of $x^{\ddagger}$). Hence, in the yellow region of the $\Delta G^{\ddagger}$ surface (Figure 2) where $x^{\ddagger}$ is confined between the values given in condition 10, simultaneous lowering of $\Delta G^{\ddagger}_{int}$ and ΔG° by the path of steepest descent will result in a late transition state relative to that observed for the corresponding nonenzymatic reaction.

INSERT: Figure 3

$$\frac{d\Delta G^{\circ}}{d\Delta G^{\ddagger}_{int}} = \left(\frac{\partial \Delta G^{\ddagger}}{\partial \Delta G^{\circ}}\right)_{\Delta G^{\ddagger}_{int}} \Bigg/ \left(\frac{\partial \Delta G^{\ddagger}}{\partial \Delta G^{\ddagger}_{int}}\right)_{\Delta G^{\circ}} = \frac{2\Delta G^{\ddagger}_{int}}{4\Delta G^{\ddagger}_{int} - \Delta G^{\circ}} \tag{6}$$

$$\left(\Delta G^{\ddagger}_{int}\right)^2 - 2\Delta G^{\circ}\Delta G^{\ddagger}_{int} + \frac{\left(\Delta G^{\circ}\right)^2}{2} = L \tag{7}$$

$$\frac{\Delta G^{\circ}}{\Delta G^{\ddagger}_{int}} = 2 \pm \sqrt{2} \tag{8}$$

$$x^{\ddagger}_{N} = \frac{6 \pm \sqrt{2}}{8} \tag{9}$$

$$\frac{6 - \sqrt{2}}{8} < x^{\ddagger}_{N} < \frac{6 + \sqrt{2}}{8} \tag{10}$$

Ketosteroid Isomerase and Mandelate Racemase. As examples, we consider the proton abstraction reactions catalyzed by ketosteroid isomerase (KSI) and mandelate racemase (MR) (scheme 2). Both enzymes have been studied as paradigms for enzymes that catalyze rapid C–H bond cleavage of carbon acids with relatively high pK_a values (Gerlt, 1998; Ha et al., 2001; Pollack et al., 1999). However, the burden borne by these enzymes is quite different. The relative reactivity of the carbon acid substrates 5-androstene-3,17-dione ($pK_a = 13$) (Hawkinson et al., 1991) and mandelate ($pK_a \approx 29$) (Gerlt et al., 1991) toward nonenzymatic proton transfer is determined primarily by their pK_a values. The ~16 unit difference between these two pK_a values corresponds to ~22 kcal/mol difference in the thermodynamic barriers to nonenzymatic deprotonation of these substrates (i.e., $\Delta\Delta G^{\circ} = -2.303RT\Delta pK_a$). However, the values of the

nonenzymatic deprotonation of these substrates (i.e., $\Delta\Delta G° = -2.303RT\Delta pK_a$). However, the values of the catalytic efficiency (k_{cat}/K_m) for KSI and MR are 3.0×10^8 $M^{-1}s^{-1}$ and 6×10^5 $M^{-1}s^{-1}$, respectively, corresponding to a 3.7 kcal/mol difference in the activation barriers for the enzyme-catalyzed reactions. Hence, KSI and MR are representative of a general trend: rather large variation of the thermodynamic barriers for proton transfers may be exhibited by nonenzymatic reactions with only limited variation of the efficiencies (k_{cat}/K_m) of the corresponding enzyme-catalyzed reactions (Richard and Amyes, 2001; Radzicka and Wolfenden, 1995).

The values of $\Delta G^{\ddagger}_{int,N}$ (13 kcal/mol) and $\Delta G°_N$ (11 kcal/mol) for the nonenzymatic, acetate-catalyzed abstraction of a proton from 5-androstene-3,17-dione were estimated by Hawkinson $et\ al$. (Hawkinson et al., 1994). For MR, the values of $\Delta G^{\ddagger}_{int,N}$ and $\Delta G°_N$ may be estimated as follows. The observed second-order rate constant ($k_2 = 13.4 \pm 0.7 \times 10^{-5}$ $M^{-1}s^{-1}$) for the imidazole-catalyzed exchange of the α-hydrogen of (R)-mandelate has been measured at 170 °C (pD 7.5) (Bearne and Wolfenden, 1997). Extrapolation of this value to 25 °C using the enthalpy of activation ($\Delta H^{\ddagger} = 29$ kcal/mol) measured by Bearne and Wolfenden (Bearne and Wolfenden, 1997) gives $k_2 = 1.6 \times 10^{-11}$ $M^{-1}s^{-1}$. Further extrapolation of this rate constant to $pK = 29$ (pK_a value of the α-proton of the mandelate anion has been estimated as ~29 (Gerlt et al., 1991)) using $\beta_e \approx 0.7$ (e.g., $\beta_e = 0.68$ and 0.88 for base-catalyzed enolization of acetophenone (Chiang et al., 1988) and acetone (Venimadhavan et al., 1989), respectively), gives an intrinsic rate constant of $k_o = 3.7 \times 10^4$ $M^{-1}s^{-1}$. Since we are not considering work terms[FOOTNOTE 1] in our analysis, we must now adjust the intrinsic rate constant to reflect reaction from an encounter complex, analogous to the enzyme-substrate complex. The equilibrium constant for formation of an encounter complex with the nucleus of a basic atom located either above or below the acidic carbon has been estimated to be approximately 0.017 M^{-1} (Hine, 1971), and adjusting the intrinsic rate constant by this factor (i.e., $k_o/0.017$ M^{-1}) gives a value of 2.2×10^6 s^{-1} corresponding to an intrinsic kinetic barrier of 9 kcal/mol. This value is in agreement with the value of 10.7 kcal/mol calculated for the intrinsic kinetic barrier for hydroxide-catalyzed proton transfers from the α-carbons of carbonyl compounds (Guthrie and Kluger, 1993; Guthrie, 1991). From the estimated pK_a value of the α-proton of mandelate and the pK_a of imidazole ($pK_a = 7.05$, (Jencks and Regenstein, 1968)), the value of $\Delta G°$ is approximately 30 kcal/mol (Gerlt, 1998). Thus, for nonenzymatic imidazole-catalyzed racemization of mandelate at 25 °C, the values of $\Delta G^{\ddagger}_{int,N}$ and $\Delta G°_N$ are approximately 9 kcal/mol and 30 kcal/mol, corresponding to $\Delta G^{\ddagger} = 30.3$ kcal/mol.

Figure 2 shows the path of steepest descent (calculated using equation 4) for lowering $\Delta G^{\ddagger}$ for both KSI and MR from the points ($\Delta G^{\ddagger}_{int,N}$, ΔG°_{N}, $\Delta G^{\ddagger}_{N}$) to $\Delta G^{\ddagger}_{E}$.[FOOTNOTE 3] The curve for MR lies at the top of the yellow region because the thermodynamic barrier for formation of an enolate from the conjugate base of a carboxylic acid is greater than that for an aldehyde, ketone, or ester. Since many carboxylate, aldehyde, ketone, or ester substrates have pK_{a} values between 13–30 (i.e., ΔG° = 18-41 kcal/mol) (Gerlt et al., 1991), and $\Delta G^{\ddagger}_{int}$ for proton abstraction from carbon acids is usually ~12 kcal/mol, most points corresponding to the nonenzymatic Marcus parameters ($\Delta G^{\ddagger}_{int,N}$, ΔG°_{N}, $\Delta G^{\ddagger}_{N}$) should lie within the yellow region shown in Figure 2 and, consequently, so will the curves corresponding the steepest descent paths between the nonenzymatic and enzymatic Marcus parameters. In addition, the position of the enzymatic transition state on the reaction coordinate will occur slightly later than that of the corresponding nonenzymatic reaction in this region. This result agrees with the "late transition state rule" proposed by Gerlt and Gassman (Gerlt and Gassman, 1993). For KSI and MR, the estimated values of $x^{\ddagger}_{N}$ are 0.605 and 0.917 while the values of $x^{\ddagger}_{E}$, determined using the path of steepest descent are 0.630 and 0.927, respectively.

Because of the high propensity of a reactive intermediate to form product, it is difficult to experimentally determine the concentrations of enzyme-bound intermediates relative to the bound substrate. To our knowledge, only one study has been conducted that compares the values of $\Delta G^{\ddagger}_{int}$ and ΔG° for an enzyme-catalyzed enolization reaction to the values of $\Delta G^{\ddagger}_{int}$ and ΔG° for its corresponding nonenzymatic reaction. Using an estimate of the dissociation constant for the wild-type KSI-intermediate complex (calculated from the dissociation constant for the D38N KSI-intermediate complex determined experimentally), Pollack and co-workers determined that K_{int} = 0.3 ± 0.2 for interconversion of bound substrate and bound intermediate (Hawkinson et al., 1994). These findings are indicated by the arrow shown in Figure 2 and support the Albery/Knowles proposal (i.e., $K_{int} \approx 1$). Whether reduction in the activation free energy barrier for a proton transfer reaction during evolution follows the path of steepest descent, or follows another path because of additional pressures of natural selection is not yet clear.[FOOTNOTE 2] Although the value of $K_{int} = 0.3$ for KSI is in agreement with expectations predicted from the results of previous studies (Hawkinson et al., 1991; Brooks and Benisek, 1994), the authors do caution that differences between their calculated and experimentally determined dissociation constant for the D38N KSI-equilenin (an intermediate analogue) complex suggest that the value of K_{int} might be corrected to 0.01.

(This corresponds to $\Delta G° = 2.73$ kcal/mol, and using equations 1 and 3 this gives $\Delta G^{\ddagger}_{int,E} = 8.88$ kcal/mol and $x^{\ddagger} = 0.538$.) Interestingly, Holman and Benisek (Holman and Benisek, 1994) concluded from their studies on KSI bearing an alanine-3-sulfinate at position 38 that Brønsted $\beta \approx 0.75$. Although this estimate of β is based on kinetics measured for only two forms of the enzyme, it does suggest a relatively late transition state consistent with the Gerlt/Gassman proposal (i.e., $K_{int} \ll 1$). Recent studies on the formation and stability of enolates of acetamide and acetate anions by Richard *et al.* (Richard et al., 2002) also suggest that enzymes can effect an increase in both the thermodynamic and kinetic stability of a bound carbanion. Certainly more experimental studies are required to clearly describe how enzymes generally alter intrinsic kinetic and thermodynamic barriers to achieve catalysis.

The evolutionary strategy discussed in the present work assumes that enzymes display no special features that selectively discriminate between the thermodynamic driving force and the intrinsic kinetic barrier for proton transfers from carbon acid substrates during the course of evolution. Because there are many examples of enzymes stabilizing bound intermediates and transition states, relative to bound reactants, as demonstrated by the potent inhibition of enzymes by intermediate and transition state analogues (Wolfenden and Frick, 1987; Radzicka and Wolfenden, 1995), one could argue that as enzymes evolve, they selectively lower $\Delta G°_E$ relative to $\Delta G^{\ddagger}_{int,E}$. In fact, much of the proficiency of an enzyme that catalyzes the reaction of a carbon acid substrate arises from the reduction of $\Delta G°$ because such enzymes often face a formidable thermodynamic barrier (i.e., large $\Delta G°$) and little advantage is to be gained by lowering the relatively small intrinsic kinetic barrier. This accounts for the tight binding of intermediate and transition state analogues. In the yellow region of Figure 2, the ratios $(\Delta G°/\Delta G^{\ddagger}_{int})$ describing the reduction in $\Delta G°$, relative to $\Delta G^{\ddagger}_{int}$, range between 0.59 and 3.41 (equation 8). For values of $\Delta G^{\ddagger}_N$ that fall within the yellow region shown in Figures 2 and 3 but close to the lower boundary, the path of steepest descent does not favor reduction of the thermodynamic barrier relative to the intrinsic kinetic barrier (e.g., for KSI (i.e., KSIa), $\Delta\Delta G°/\Delta\Delta G^{\ddagger}_{int} \approx 0.65$). However, for $\Delta G^{\ddagger}_N$ values that lie close to the upper boundary of the yellow region on the contour plot where the contour lines have more curvature, reduction of the thermodynamic barrier is favored relative to the intrinsic kinetic barrier (e.g., for MR, $\Delta\Delta G°/\Delta\Delta G^{\ddagger}_{int} \approx 3.27$). Interestingly, this degree of discrimination is similar to that found experimentally for KSI (slope of arrow shown in Figure 2 (i.e., KSIb), $\Delta\Delta G°/\Delta\Delta G^{\ddagger}_{int} \approx 3.43$). For those enzymes that catalyze abstraction of the α-proton from a carbon acid substrate with a high pK_a value (i.e., when $\Delta G^{\ddagger}_N$ is dominated by $\Delta G°_N$

as is the case with MR), preferential reduction in $\Delta G°$ is most advantageous. Indeed, for values of $\Delta G^{\ddagger}_N$ where $\Delta G°_N > 2\Delta G^{\ddagger}_{int,N}$, the path of steepest descent will result in enhanced differential binding such that $\Delta G°$ will be reduced to a greater extent than $\Delta G^{\ddagger}_{int}$ (i.e., $d\Delta G°/d\Delta G^{\ddagger}_{int} > 1$; see equation 6). Although the results of the single study using KSI do not appear to support the path of steepest descent as a course of evolution, it may be that for more proficient enzymes such as MR, the reduction of both $\Delta G°$ and $\Delta G^{\ddagger}_{int}$ more closely follows the path of steepest descent during evolution.

At present, it is not possible to describe a general trend for the reduction of $\Delta G°$ relative to $\Delta G^{\ddagger}_{int}$ over the course of evolution because of the paucity of experimental studies that specifically measure the intrinsic kinetic barriers of enzyme-catalyzed reactions. However, the present analysis does provide an alternative framework for thinking about the application of Marcus formalism to enzymatic reactions.

3.   Conclusions

The free energy of activation for the nonenzymatic formation of an enolate ion is dominated by a large thermodynamic barrier ($\Delta G°$) and consequently, $x^{\ddagger}$ occurs late on the reaction coordinate. For an enzyme that has evolved by decreasing $\Delta G^{\ddagger}$ for an enolization reaction by following the path of steepest descent on the $\Delta G^{\ddagger}$ two-dimensional surface, as defined by Marcus formalism, the values of the intrinsic kinetic ($\Delta G^{\ddagger}_{int,E}$) and thermodynamic ($\Delta G°_E$) barriers for proton transfer reactions on the enzyme may be predicted using the known values from the corresponding nonenzymatic reaction ($\Delta G^{\ddagger}_{int,N}$ and $\Delta G°_N$) and the free energy of activation on the enzyme ($\Delta G^{\ddagger}_E$). The values of $\Delta G^{\ddagger}_{int,E}$ and $\Delta G°_E$, determined in such a manner, correspond to a position for the enzymatic transition state on the reaction coordinate that is later than that for the corresponding nonenzymatic transition state if condition 10 is satisfied. Since the values of $\Delta G^{\ddagger}_{int,N}$ and $\Delta G°_N$ for most nonenzymatic enolization reactions are expected to satisfy condition 10, enzymes catalyzing the corresponding reactions will also have late transition states if $\Delta G^{\ddagger}$ for the proton transfer step associated with substrate enolization has been decreased following the path of steepest descent. The path of steepest descent favors reduction of $\Delta G°$ relative to $\Delta G^{\ddagger}_{int}$ when $\Delta G°_N$ dominates (i.e., $\Delta G°_N > 2\Delta G^{\ddagger}_{int,N}$) the activation free energy for the nonenzymatic reaction ($\Delta G^{\ddagger}_N$).

Acknowledgements

Footnotes

Footnote 1: For higher-order reactions such as bimolecular and termolecular reactions involving general acidic or general basic catalysts, Marcus formalism can only be applied to the encounter complex of the reacting species, unless the free energy change associated with formation of the encounter complex, known as the work term (w_r), is also included in the analysis (i.e., $\Delta G^{\ddagger}_{obs} = \Delta G^{\ddagger} + w_r$). For this reason, the present analysis is restricted to comparisons between enzyme-bound species and an encounter complex between the general acidic or general basic catalyst and the substrate for the corresponding nonenzymatic reaction.

We recognize that Marcus theory does have a major limitation because the reaction coordinate is assumed to depend on just one variable. Most molecular reactions involve two or more reaction events whose relative progress along the reaction coordinate varies for different members of a reaction series (Grunwald, 1985). Marcus theory has been expanded upon by the introduction of additional progress variables for each independently variable reaction event; however, such multidimensional Marcus formalisms are not discussed in the present work and the analysis is presented in terms of one-dimensional Marcus theory (Grunwald, 1985; Guthrie, 1996).

Footnote 2: There are many factors that affect enzyme evolution including local substrate concentrations, levels of enzyme expression, enzyme concentration, flux of the metabolic pathway that contains the enzyme, barriers to enzyme flexibility, as well as the activation barriers associated with chemical steps (Keleti and Welch, 1984; Pettersson, 1989). The present argument applies only to evolutionary pressure to lower a rate-limiting proton transfer reaction on an enzyme.

Footnote 3: No single step of the catalytic cycle of KSI or MR appears to be solely rate-limiting. For KSI, enolization, ketonization, and product dissociation are each partially rate-limiting (Hawkinson et al., 1991; Brooks and Benisek, 1994; Holman and Benisek, 1994; Xue et al., 1990). The rate of MR catalysis is partially limited by diffusion (St. Maurice and Bearne, 2002). Hence, the values of $\Delta G^{\ddagger}_E$ used in our analysis are the free energies of activation associated with deprotonation of the *bound* substrate (i.e., 10.3 kcal/mol for 5-androstene-3,17-dione (Hawkinson et al., 1991) and 13.4 kcal/mol for (*R*)-mandelate (St. Maurice and Bearne, 2002); see Figure 2).

References

1. Richard, J. P., Amyes, T. L. (2001) Proton transfer at carbon. Curr. Opin. Chem. Biol. 5, 626-633.

2. Kluger, R. (1990) Ionic intermediates in enzyme-catalyzed carbon-carbon bond formation: patterns, prototypes, probes, and proposals. Chem. Rev. 90, 1151-1169.

3. Gerlt, J. A. (1998) in Bioorganic Chemistry: Peptides and Proteins (Hecht, S. M., ed.), Oxford University Press, New York, pp. 279-311.

4. Albery, W. J. (1980) The Application of the Marcus Relation to Reactions in Solution. Ann. Rev. Phys. Chem. 31, 227-263.

5. Cohen, A. O., Marcus, R. A. (1968) Slope of free energy plots in chemical kinetics. J. Phys. Chem. 72, 4249-4256.

6. Marcus, R. A. (1969) Unusual slopes of free energy plots in kinetics. J. Am. Chem. Soc. 91, 7224-7225.

7. Kresge, A. J., Silverman, D. N. (1999) Application of Marcus Rate Theory to Proton Transfer in Enzyme-Catalyzed Reactions. Methods Enzymol. 308, 276-297.

8. Silverman, D. N. (2000) Marcus rate theory applied to enzymatic proton transfer. Biochim. Biophys. Acta 1458, 88-103.

9. Maskill, H. (1985) The physical basis of organic chemistry, Oxford University Press, New York

10. Amyes, T. L., Richard, J. P. (1996) Determination of the pKa of Ethyl Acetate: Brønsted Correlation for Deprotonation of a Simple Oxygen Ester In Aqueous Solution. J. Am. Chem. Soc. 118, 3129-3141.

11. Chiang, Y., Kresge, A. J., Schepp, N. P., Xie, R.-Q. (2000) Generation of the Enol of Methyl Mandelate by Flash Photolysis of Methyl Phenyldiazoacetate in Aqueous Solution and Study of Rates of Ketonization of This Enol in That Medium. J. Org. Chem. 65, 1175-1180.

12. Richard, J. P., Williams, G., O'Donoghue, A. C., Amyes, T. L. (2002) Formation and Stability of Enolates of Acetamide and Acetate Anion: An Eigen Plot for Proton Transfer at α-Carbonyl Carbon. J. Am. Chem. Soc. 124, 2957-2968.

13. Thibblin, A., Jencks, W. P. (1979) Unstable Carbanions. General Acid Catalysis of the Cleavage of 1-Phenylcyclopropanol and 1-Phenyl-2-arylcyclopropanol Anions. J. Am. Chem. Soc. 101, 4963-4973.

14. Guthrie, J. P., Kluger, R. (1993) Electrostatic stabilization can explain the unexpected acidity of carbon acids in enzyme-catalyzed reactions. J. Am. Chem. Soc. 115, 11569-11572.

15. Albery, W. J. (1982) Application of the Marcus Relation to Concerted Proton Transfers. J. Chem. Soc. Faraday Trans. 1 78, 1579-1590.

16. Chiang, Y., Kresge, A. J., Santaballa, J. A., Wirz, J. (1988) Ketonization of Acetophenone Enol in Aqueous Buffer Solutions. Rate-Equilibrium Relations and Mechanism of the "Uncatalyzed" Reaction. J. Am. Chem. Soc. 110, 5506-5510.

17. Eigen, M. (1964) Proton Transfer, Acid-Base Catalysis, and Enzymatic Hydrolysis. Angew. Chem. Int. Ed. Engl. 3, 1-72.

18. Bernasconi, C. F. (1992) The Principle of Non-perfect Synchronization. Adv. Phys. Org. Chem. 27, 119-238.

19. Guthrie, J. P. (1998) Predicting the rates of proton transfer reactions: a simple model using equilibrium constants and distortion energies. J. Phys. Org. Chem. 11, 632-641.

20. Gerlt, J. A., Gassman, P. G. (1993) Understanding the rates of certain enzyme-catalyzed reactions: proton abstraction from carbon acids, acyl-transfer reactions, and displacement reactions of phosphodiesters. Biochemistry 32, 11943-11952.

21. Gerlt, J. A., Gassman, P. G. (1993) An explanation for rapid enzyme-catalyzed proton abstraction from carbon acids: importance of late transition states in concerted mechanisms. J. Am. Chem. Soc. 115, 11552-11568.

22. Gerlt, J. A., Gassman, P. G. (1992) Understanding Enzyme-Catalyzed Proton Abstraction from Carbon Acids: Details of Stepwise Mechanisms for β-Elimination Reactions. J. Am. Chem. Soc. 114, 5928-5934.

23. Gerlt, J. A., Kreevoy, M. M., Cleland, W., Frey, P. A. (1997) Understanding enzymic catalysis: the importance of short, strong hydrogen bonds. Chem. Biol. 4, 259-267.

24. Albery, W. J., Knowles, J. R. (1977) Efficiency and Evolution in Enzyme Catalysis. Angew. Chem. Int. Ed. Engl. 16, 285-293.

25. Burbaum, J. J., Raines, R. T., Albery, W. J., Knowles, J. R. (1989) Evolutionary optimization of the catalytic effectiveness of an enzyme. Biochemistry 28, 9293-305.

26. Albery, W. J., Knowles, J. R. (1976) Evolution of Enzyme Function and the Development of Catalytic Efficiency. Biochemistry 15, 5631-5640.

27. Chin, J. (1983) Perfect Enzymes: Is the Equilibrium Constant between the Enzyme's Bound Species Unity? J. Am. Chem. Soc. 105, 6502-6503.

28. Stackhouse, J., Nambiar, K. P., Burbaum, J. J., Stauffer, D. M., Benner, S. A. (1985) Dynamic Transduction of Energy and Internal Equilibria in Enzymes: A Reexamination of Pyruvate Kinase. J. Am. Chem. Soc. 107, 2757-2763.

29. Gerlt, J. A., Kozarich, J. W., Kenyon, G. L., Gassman, P. G. (1991) Electrophilic Catalysis Can Explain the Unexpected Acidity of Carbon Acids in Enzyme-Catalyzed Reactions. J. Am. Chem. Soc. 113

30. Hanson, K. R., Rose, I. A. (1975) Interpretations of Enzyme Reaction Stereospecificity. Acc. Chem. Res. 8, 1-10.

31. Hammond, G. S. (1955) A correlation of reaction rates. J. Am. Chem. Soc. 77, 334-338.

32. Yadav, A., Jackson, R. M., Holbrook, J. J., Warshel, A. (1991) Role of Solvent Reorganization Energies in the Catalytic Activity of Enzymes. J. Am. Chem. Soc. 113, 4800-4805.

33. Ha, N.-C., Choi, G., Choi, K. Y., Oh, B.-H. (2001) Structure and enzymology of Δ^5-3-ketosteroid isomerase. Curr. Opin. Struct. Biol. 11, 674-678.

34. Pollack, R. M., Thornburg, L. D., Wu, Z. R., Summers, M. F. (1999) Mechanistic Insights from the Three-Dimensional Structure of 3-Oxo-Δ^5-steroid Isomerase. Arch. Biochem. Biophys. 370, 9-15.

35. Hawkinson, D. C., Eames, T. C. M., Pollack, R. M. (1991) Energetics of 3-Oxo-Δ^5-steroid Isomerase: Source of the Catalytic Power of the Enzyme. Biochemistry 30, 10849-10858.

36. Radzicka, A., Wolfenden, R. (1995) A proficient enzyme. Science 267, 90-93.

37. Hawkinson, D. C., Pollack, R. M., Ambulos, N. P. (1994) Evaluation of the Internal Equilibrium Constant for 3-Oxo-Δ^5-steroid Isomerase Using the D38E and D38N Mutants: The Energetic Basis for Catalysis. Biochemistry 33, 12172-12183.

38. Bearne, S. L., Wolfenden, R. (1997) Mandelate racemase in pieces: effective concentrations of enzyme functional groups in the transition state. Biochemistry 36, 1646-1656.

39. Venimadhavan, S., Shelly, K. P., Stewart, R. (1989) Catalysis of the Enolization of Acetone by Mono- and Dicarboxylate Bases. The Role of Hydrogen Bonding. J. Org. Chem. 54, 2483-2485.

40. Hine, J. (1971) Rate and Equilibrium in the Addition of Bases to Electrophilic Carbon and in S$_N$1 Reactions. J. Am. Chem. Soc. 93, 3701-3708.

41. Guthrie, J. P. (1991) Rate-Equilibrium Correlations for the Aldol Condensation: An Analysis in Terms of Marcus Theory. J. Am. Chem. Soc. 113, 7249-7255.

42. Jencks, W. P., Regenstein, J. (1968) in Handbook of Biochemistry (Sober, H. A., ed.), The Chemical Rubber Co., Cleveland, OH, pp. J150-J189.

43. Brooks, B., Benisek, W. F. (1994) Mechanism of the Reaction Catalyzed by the Δ^5-3-Ketosteroid Isomerase of *Comamonas* (*Pseudomonas*) *testosteroni*: Kinetic Properties of a Modified Enzyme in Which Tyrosine 14 Is Replaced by 3-Fluorotyrosine. Biochemistry 33, 2682-2687.

44. Holman, C. M., Benisek, W. F. (1994) Extent of Proton Transfer in the Transition States of the Reaction Catalyzed by the Δ^5-3-Ketosteroid Isomerase of *Comamonas* (*Pseudomonas*) *testosteroni*: Site-Specific Replacement of the Active Site Base, Aspartate 38, by the Weaker Base Alanine-3-sulfinate. Biochemistry 33, 2672-2681.

45. Wolfenden, R., Frick, L. (1987) in Enzyme Mechanisms (Page, M. I.,Williams, A., eds.), Royal Society of Chemistry, London, pp. 97-122.

46. Radzicka, A., Wolfenden, R. (1995) Transition State and Multisubstrate Analog Inhibitors. Methods Enzymol. 249, 284-312.

47. Grunwald, E. (1985) Structure-Energy Relations, Reaction Mechanism, and Disparity of Progress of Concerted Reaction Events. J. Am. Chem. Soc. 107, 125-133.

48. Guthrie, J. P. (1996) Multidimensional Marcus Theory: An Analysis of Concerted Reactions. J. Am. Chem. Soc. 118, 125-133.

49. Keleti, T., Welch, G. R. (1984) The evolution of enzyme catalytic power. Biochem. J. 223, 299-303.

50. Pettersson, G. (1989) Effect of evolution on the kinetic properties of enzymes. Eur. J. Biochem. 184, 561-566.

51. Xue, L., Talalay, P., Mildvan, A. S. (1990) Studies on the Mechanism of the Δ^5-3-Ketosteroid Isomerase Reaction by Substrate, Solvent, and Combined Kinetic Deuterium Isotope Effects on Wild-Type and Mutant Enzymes. Biochemistry 29, 7491-7500.

52. St. Maurice, M., Bearne, S. L. (2002) Kinetics and thermodynamics of mandelate racemase catalysis. Biochemistry 41, 4048-4058.

Figure Legends

Figure 1. Dependence of G on the position of the reaction coordinate, x, for the nonenzymatic and enzyme-catalyzed enolization of a carbon acid. The free energy difference between the enolic(ate) intermediate (at $x = 1$) and the substrate carbon acid (at $x = 0$) is $\Delta G°$. Curve A is for the nonenzymatic (imidazole-catalyzed) racemization of mandelate and was calculated using equation 2 with values of $\Delta G^{\ddagger}_{int}$ = 9 kcal/mol and $\Delta G° = 30$ kcal/mol (see text). Curve B corresponds to the scenario in which the overall activation barrier $\Delta G^{\ddagger}$ is lowered on MR (to 13.4 kcal/mol) by simultaneous lowering of $\Delta G°$ (to 13.3 kcal/mol) and $\Delta G^{\ddagger}_{int}$ (to 3.91 kcal/mol) by the path of steepest descent (see Figure 2). This scenario is similar to that proposed by Gerlt and Gassman (Gerlt and Gassman, 1993) in which the enzymatic transition state occurs late on the reaction coordinate. Curves C and D show different degrees of differential binding as proposed by Albery and Knowles (Albery and Knowles, 1976). For curve C, the enzyme has reduced the overall activation barrier $\Delta G^{\ddagger}$ by only lowering $\Delta G°$ (to 8.0 kcal/mol). Curve D illustrates the case where $\Delta G° = 0$ and $\Delta G^{\ddagger} = \Delta G^{\ddagger}_{int}$. For all curves, the values of G have been normalized so that $G = 0$ when $x = 0$ (i.e., ($\Delta G^{\ddagger}_{int} + \Delta G°/2$) is added to each value of G calculated using equation 2).

Figure 2. Level curves for the activation free energy surface described by equation 1 and paths of steepest descent for reduction of $\Delta G^{\ddagger}$. Values graphed are for endergonic proton transfer reactions (i.e., $\Delta G° > 0$) with $|\Delta G°| \leq 4\Delta G^{\ddagger}_{int}$. For the enzyme-catalyzed reactions, the values of $\Delta G^{\ddagger}_{E}$ are 10.3 kcal/mol and 13.4 kcal/mol for KSI (Hawkinson et al., 1994) and MR (St. Maurice and Bearne, 2002), respectively. The estimated values of ($\Delta G^{\ddagger}_{int,N}$, $\Delta G°_{N}$, $\Delta G^{\ddagger}_{N}$) (in kcal/mol) for the corresponding nonenzymatic reactions, are (13, 11, 19.1) (Hawkinson et al., 1994) and (9, 30, 30.3), respectively (see text). The curves between the filled circles, calculated using equation 4, show the paths of steepest descent from $\Delta G^{\ddagger}_{N}$ (labeled N) to $\Delta G^{\ddagger}_{E}$ (labeled E); their intersection with the level curves at the observed $\Delta G^{\ddagger}_{E}$ values gives the values (in kcal/mol) of ($\Delta G^{\ddagger}_{int,E}$, $\Delta G°_{E}$) as (6.48, 6.76) and (3.91, 13.35) for KSI (labeled KSIa) and MR, respectively. In the region shaded yellow, the path of steepest descent yields $x^{\ddagger}_{E} > x^{\ddagger}_{N}$, whereas in the blue region it yields $x^{\ddagger}_{E} < x^{\ddagger}_{N}$. The arrow (labeled KSIb) shows experimental results obtained for KSI by Hawkinson *et al*. (Hawkinson et al., 1994) where the observed values (in kcal/mol) of $\Delta G^{\ddagger}_{int,E}$ and $\Delta G°_{E}$ are 10 and 0.7, respectively. (Note that this *activation free energy surface* differs from the traditional standard molar *free energy reaction maps* which plot different reaction coordinates on the x-axis and y-axis with the

free energy (G) being plotted on the z-axis (Maskill, 1985). Only the saddle point on these maps is the free energy of activation ($\Delta G^{\ddagger}$).)

Figure 3. Gradient vector field graph for $\Delta G^{\ddagger}$ (equation 1). The red lines extending from the origin have slopes equal to specific ratios of $\Delta G^{\ddagger}_{int}/\Delta G^{\circ}$ (i.e., corresponding to constant values of $x^{\ddagger}$ shown in red). The vectors are normalized to unit length.

Scheme 1. General base-catalyzed enolate formation.
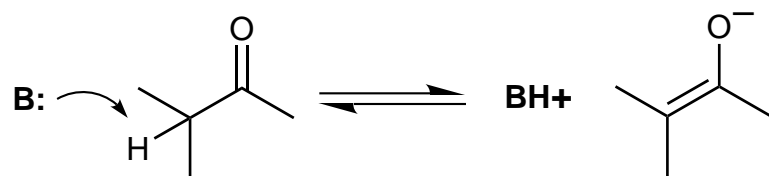
Scheme 2. Reactions catalyzed by KSI (**A**) and MR (**B**).

A.

5-androstene-3,17-dione

Tyr 14-OH
COOH
Asp 99

Asp 38

Tyr 14-OH
COOH
Asp 99

Asp 38

4-androstene-3,17-dione

Tyr 14-OH
COOH
Asp 99

Asp 38

B.

Glu 317

B_1: HB_2

(*R*)-mandelate

Glu 317

B_1H HB_2

aci-carboxylate
intermediate

Glu 317

B_1H :B_2

(*S*)-mandelate
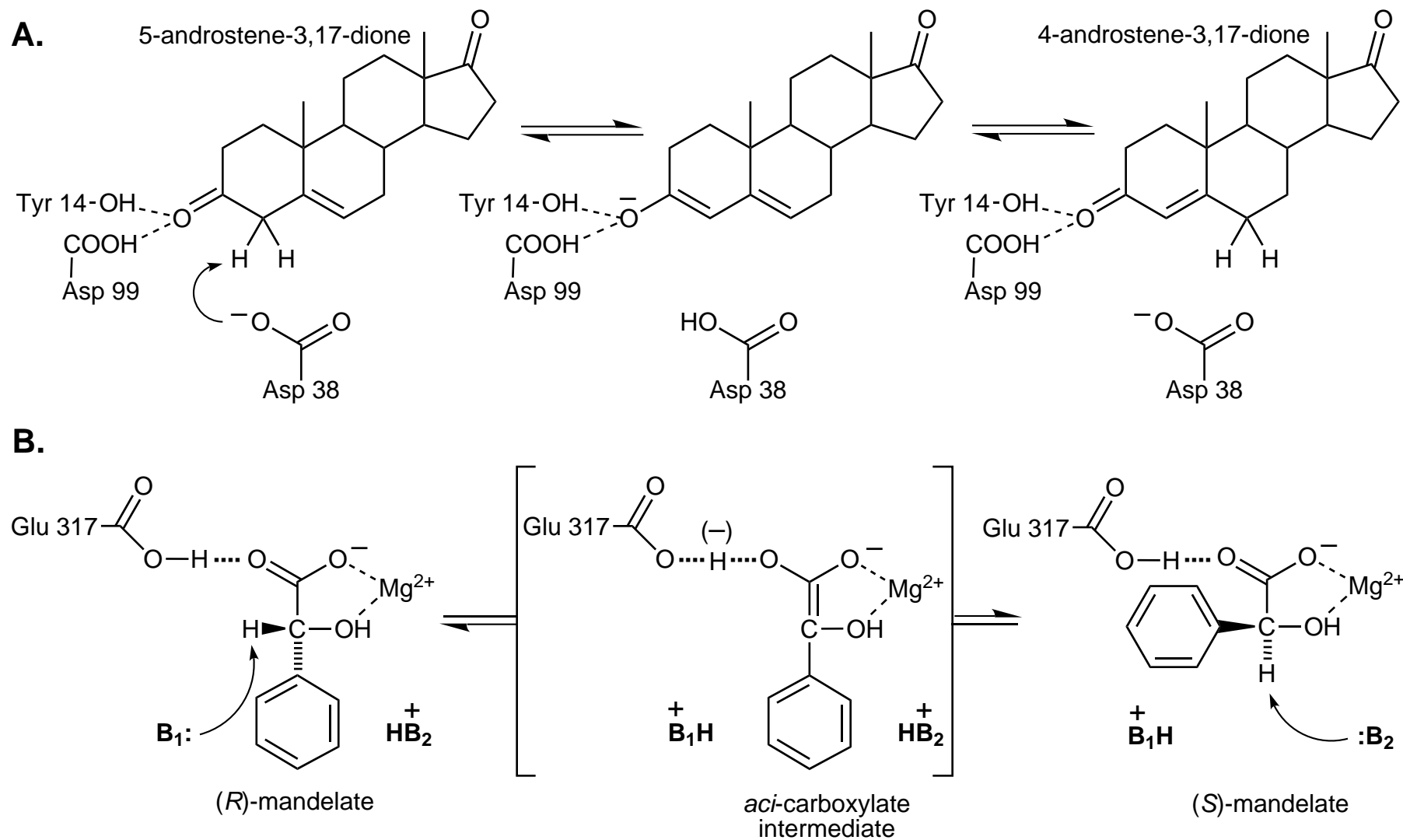
B$_1$ and **B$_2$** represent the active site bases His 297 and Lys 166, respectively.

21
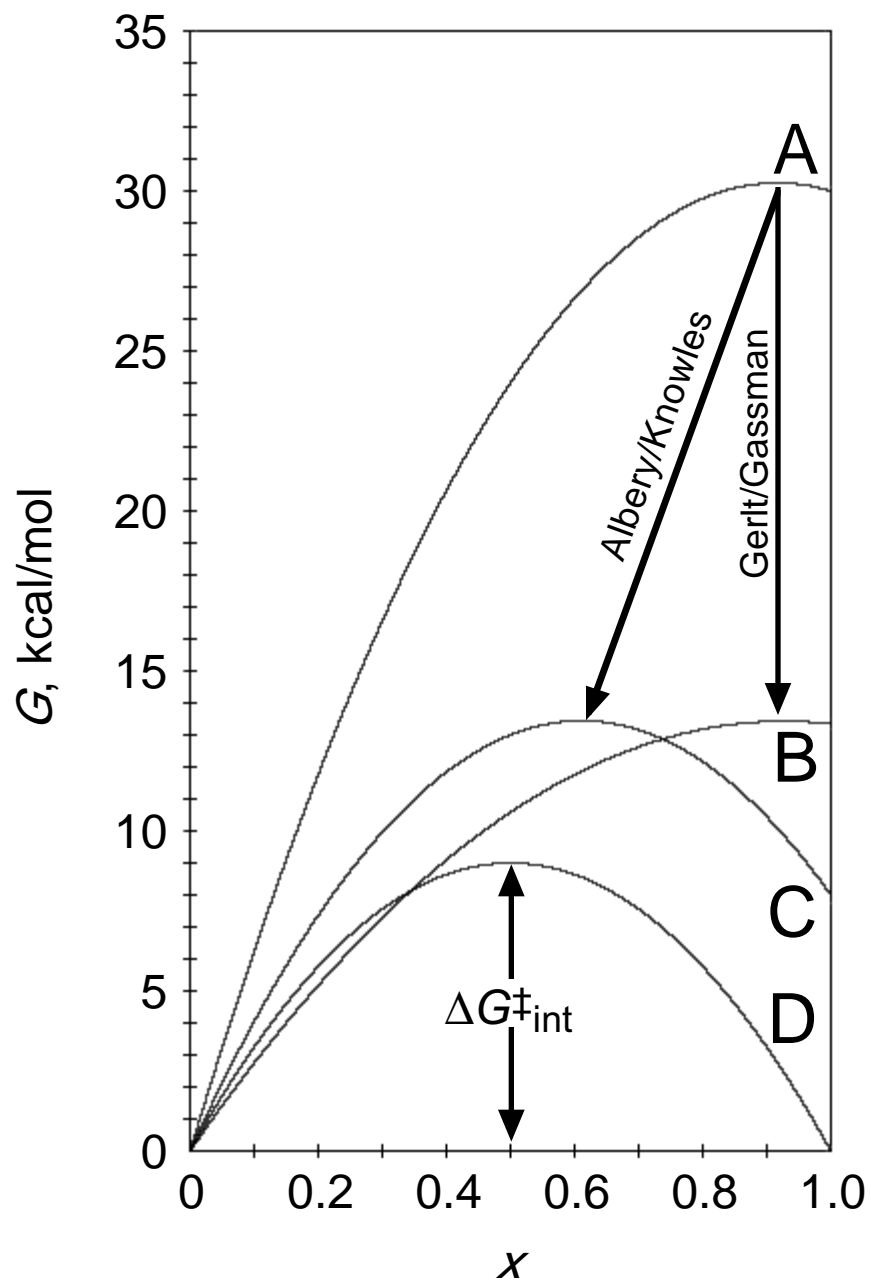
Bearne & Spiteri – Figure 1
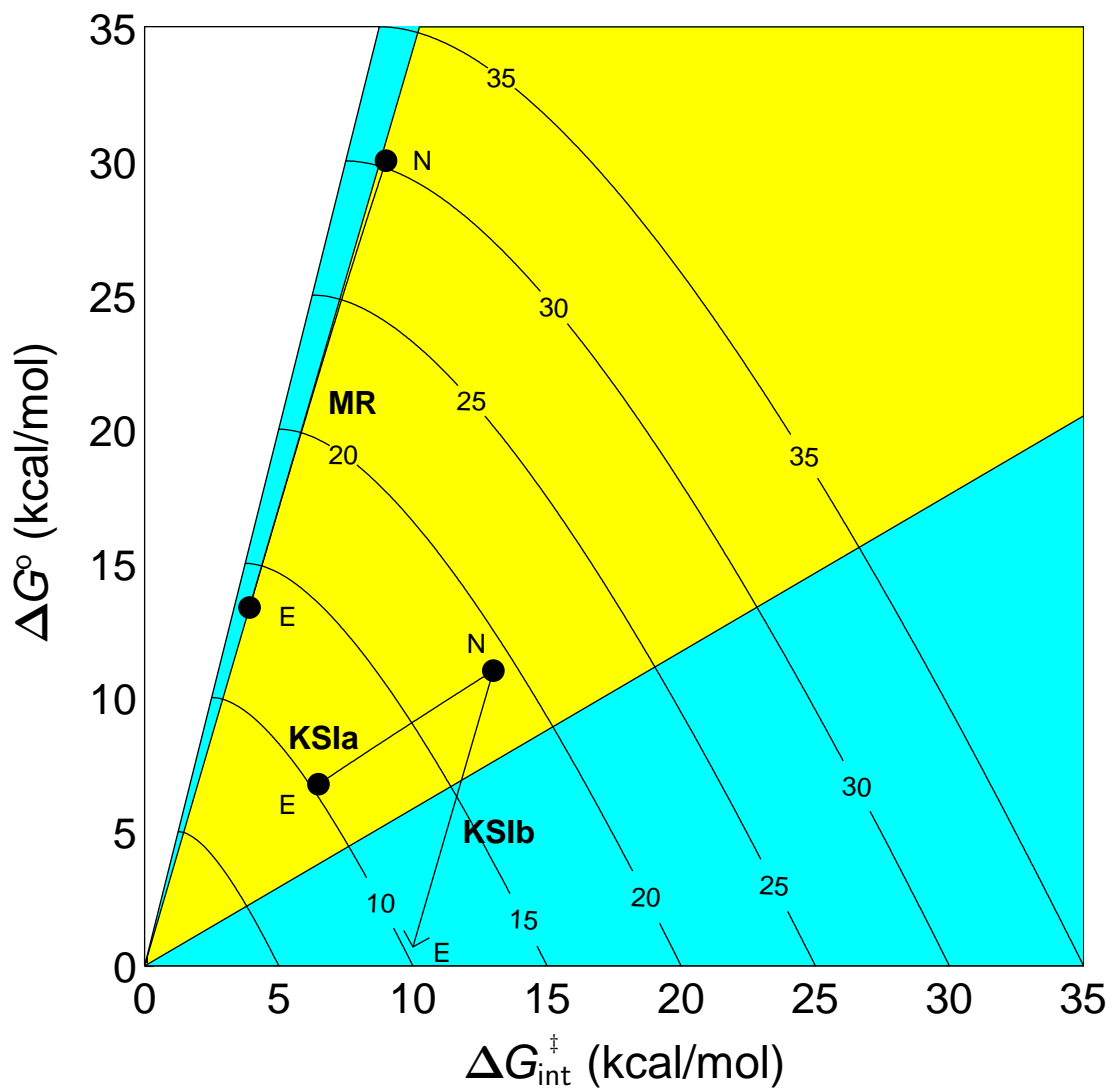
Bearne & Spiteri – Figure 2

Bearne & Spiteri – Figure 3